Proceedings of A. Razmadze
Mathematical Institute
Vol. **158** (2012), 99–112

THE EFFECT OF THE GAP WIDTH ON THE INSTABILITY AND BIFURCATION OF FLOWS BETWEEN TWO ROTATING POROUS CYLINDERS

L. SHAPAKIDZE

Abstract. The stability of viscous heat-conducting flows between two rotating porous cylinders has been examined for various width values of the gap between the cylinders. The paper presents the results of investigation of the neutral curves which separate the instability regions from the stability ones, also the regimes arising after the main flow loses stability.

რეზიუმე. შესწავლილია ბლანტი სითბოგამტარი სითხის მდგრადობის ამოცანა სხვადასხვა მანძილით დაშორებულ ფოროვან ცილინდრებს შორის. წარმოდგენილია მდგრადი არის არამდგრადი არისაგან გამყოფი ნეიტრალური მრუდები და შესწავლილია ის მოძრაობები, რომლებიც წარმოიშვებიან ძირითადი დინების მდგრადობის დაკარგვის შედეგად.

1. Introduction

One of the generalizations of the classical Couette-Taylor problem is the problem on the stability of a nonisothermal flow between two rotating permeable cylinders, on which a radial flow and a radial temperature gradient are superposed. This type of flow occurs in technical hydrodynamics in connection with the problem of filtration and is of special interest.

In the recent paper [1] where this problem is investigated, we used numerical analysis to construct complex flow regimes near bifurcations at which vortical and azimuthal waves originate. It is assumed there that the porous cylinders are heated up to different temperatures and the radius of the outer cylinder is twice as that of the inner cylinder.

In the present paper we study the effect of various width values of the gap between cylinders on the stability and bifurcation of the above-mentioned nonizothermal flow.

2010 *Mathematics Subject Classification.* 76E07, 76U05.

Key words and phrases. Nonizothermal flow, permeable cylinders, bifurcation, complex regimes.

2. Formulation of the Problem

Let a viscous heat-conducting fluid fill the cavity between two rotating permeable cylinders heated up to different temperatures. We denote the radii, angular velocities and temperatures of the internal and the outer cylinder by R_1, Ω_1, Θ_1 and R_2, Ω_2, Θ_2, respectively. It is assumed that external mass forces are absent, the velocity of the flow through the cylinder cavity cross-section is equal to zero, and the fluid inflow through the walls of one cylinder is equal to the fluid outflow through the walls of the other.

Let the scales of length, velocity, time, temperature, pressure and density be denoted, respectively, by R_1, $\Omega_1 R_1$, $1/\Omega_1$, Θ_1, $\nu\rho'\Omega_1$, the density scale be as the fluid density at the temperature Θ_1. Using the dimensionless system of Navier-Stokes, heat transfer, continuity equations and an equation of state [2], under the above assumptions we obtain - in terms of cylindrical coordinates (r, φ, z) with the z-axis coinciding with that of the cylinders - the following exact solution with the velocity vector $\boldsymbol{V}_0 = \{v_{0r}(r), v_{0\varphi}(r), 0\}$, temperature T_0, pressure Π_0 :

$$v_{0r} = \frac{\varkappa}{\mathrm{Re}\, r}, \quad v_{0\varphi} = \begin{cases} ar^{\varkappa+1} + \dfrac{b}{r}, & \varkappa \neq 2, \\ \dfrac{a_1 \ln r + 1}{r}, & \varkappa = -2, \end{cases} \qquad T_0 = c_1 + c_2 r^{\varkappa \mathrm{Pr}}, \tag{2.1}$$

$$\Pi_0 = \int_1^r \left(\frac{v_{0\varphi}^2}{r} - \frac{\varkappa^2}{\mathrm{Re}^2 r^3} \right) \Big[1 - \frac{Ra}{\mathrm{Pr}} (r^{\varkappa \mathrm{Pr}} - 1) \Big] dr + \mathrm{const},$$

where

$$a = \frac{\Omega R^2 - 1}{R^{\varkappa+2} - 1}, \quad b = 1 - a, \quad a_1 = \frac{\Omega R^2 - 1}{\ln R}, \quad c_2 = \frac{1 - \Theta}{1 - R^{\varkappa \mathrm{Pr}}},$$
$$c_1 = 1 - c_2, \quad \Theta = \frac{\Theta_2}{\Theta_1}, \quad R = \frac{R_2}{R_1}, \quad \Omega = \frac{\Omega_2}{\Omega_1},$$

$Ra = \beta \Theta_1 c_2 \mathrm{Pr}$ is the Rayleigh number, $\mathrm{Re} = \frac{\Omega_1 R_1^2}{\nu}$ is the Reynolds number, $\mathrm{Pr} = \frac{\nu}{\chi}$ is the Prandtl number, while ν, χ, β are, respectively, the coefficients of kinematic viscosity, thermal diffusion and thermal expansion; $\varkappa = u_1 \mathrm{Re} = u_2 \mathrm{Re}\, R$ is the radial Reynolds number, and u_1, u_2 are the radial velocities at $r = 1$, $r = R$, respectively. The radial flow is inward for $\varkappa < 0$ and outward for $\varkappa > 0$.

Note that in the case of inward flow $\varkappa < 0$ we observe that for $\Theta_2 < \Theta_1$ (i.e., the temperature of the inner cylinder is greater than that of the outer cylinder), $Ra > 0$; for $\Theta_2 > \Theta_1$ (i.e., the temperature of the outer cylinder is greater than that of the inner cylinder), $Ra < 0$. Conversely, for the outward flow $\varkappa > 0$ the situation is as follows: for $\Theta_2 > \Theta_1$ (i.e., the temperature of the outer cylinder is greater than that of the inner cylinder), $Ra > 0$; for

$\Theta_2 < \Theta_1$ (i.e.the temperature of the inner cylinder is greater than that of the outer cylinder), $Ra < 0$.

The flow with velocity vector $\boldsymbol{V}_0$, temperature T_0, pressure Π_0 is called the main stationary flow [1].

The aim of this study is to calculate - taking into account both axially symmetric and oscillation three-dimensional perturbations - the neutral curves which separate the instability regions from the stability ones for various width values of the gap between the cylinders. Also, we investigate the regimes arising after the main flows lose their stability.

3. Neutral Curves

We consider the first stability loss with secondary regimes branching off the main flow for various width values of the gap between the cylinders.

Perturbations of the main flow are defined by means of the nonlinear system of equations written in terms of vector functions $\boldsymbol{F} = \{v_r, v_\varphi, v_z, T\}$ and $\boldsymbol{F}_1 = \{u_r, u_\varphi, u_z, T_1\}$, where v_r, v_φ, v_z, T are perturbation velocity and temperature components [1]:

$$\begin{gathered}\frac{\partial \boldsymbol{F}}{\partial t} + N\boldsymbol{F} - \frac{1}{\mathrm{Re}}\,\boldsymbol{M}\boldsymbol{F} + \frac{1}{\mathrm{Re}}\,\nabla_1\Pi = -\mathcal{L}(\boldsymbol{F},\boldsymbol{F}),\\ (\nabla_1, r\boldsymbol{F}) = 0, \quad \boldsymbol{F}\big|_{r=1,R} = 0,\end{gathered} \tag{3.1}$$

where

$$\begin{gathered}\boldsymbol{M}\boldsymbol{F} = \Big\{\Delta_1 v_r - \frac{1-\varkappa}{r^2}\,v_r - \frac{2}{r^2}\frac{\partial v_\varphi}{\partial \varphi}, \Delta_1 v_\varphi - \frac{1+\varkappa}{r^2}v_\varphi + \\ + \frac{2}{r^2}\frac{\partial v_r}{\partial \varphi}, \Delta_1 v_z, \frac{1}{\mathrm{Pr}}\Delta_1 T\Big\},\\ \boldsymbol{N}\boldsymbol{F} = \omega_1\frac{\partial \boldsymbol{F}}{\partial \varphi} + \Big\{Ra\omega_2 T - 2\omega_1 v_\varphi, -g_1 v_r, 0, \frac{g_2}{\mathrm{Pr}}v_r,\Big\},\\ \mathcal{L}(\boldsymbol{F},\boldsymbol{F}_1) = \Big\{\boldsymbol{F},\nabla_1)u_r - \frac{v_\varphi u_\varphi}{r},\ (\boldsymbol{F},\nabla_1)u_\varphi + \frac{v_r u_\varphi}{r}, (\boldsymbol{F},\nabla_1)u_z, (\boldsymbol{F},\nabla_1)T_1\Big\},\\ \Delta_1 = \frac{\partial^2}{\partial r^2} + \frac{1-\varkappa}{r}\,\frac{\partial}{\partial r} + \frac{1}{r^2}\,\frac{\partial^2}{\partial \varphi^2} + \frac{\partial^2}{\partial z^2}\,, \quad \nabla_1 = \Big\{\frac{\partial}{\partial r}, \frac{1}{r}\frac{\partial}{\partial \varphi}, \frac{\partial}{\partial z}, 0\Big\},\\ g_1(r) = \frac{dv_{0\varphi}}{dr} + \frac{v_{0\varphi}}{r}, \quad \omega_1 = \frac{v_{0\varphi}}{r}, \quad \omega_2 = \omega_1^2 r, \quad g_2 = \varkappa r^{\varkappa\mathrm{Pr}-1}.\end{gathered}$$

The system of equations (3.1) is written in terms of the Boussinesq approximation [3], where $\beta\theta_1 \ll 1$. It is assumed that the velocity of the flow through the cylinder walls is such that it is not influenced by perturbations arising in the fluid between the two cylinders. In the sequel, it is always assumed that the velocity, temperature and pressure components are periodic with respect to z and φ with the known periods $2\pi/\alpha$ and $2\pi/m$, respectively.

The neutral curves corresponding to bifurcations generated by vortices are found by solving the linear spectral problem obtained by the perturbation equation (3.1)

$$\begin{gathered}(\boldsymbol{M}-\operatorname{Re}\boldsymbol{N})\Phi_0=\nabla_1 p_0,\\ (\nabla_1, r\Phi_0)=0,\quad \Phi_0|_{r=1,R}=0,\end{gathered}\tag{3.2}$$

where

$$\Phi_0=\big\{u_0(r),v_0(r),iw_0(r),\tau_0(r)\big\}e^{i\alpha z},\quad p_0=q_0(r)e^{i\alpha z}.\tag{3.3}$$

The substitution of (3.3) into (3.2) gives, after dividing the variables in (3.2), the following spectral problem for ordinary differential equations

$$\begin{gathered}\Big(L-\frac{1-\varkappa}{r^2}-\alpha^2\Big)u_0=\frac{dq_0}{dr}-2\operatorname{Re}\omega_1 v_0+\operatorname{Re}Ra\omega_2\tau_0,\\ \Big(L-\frac{1+\varkappa}{r^2}-\alpha^2\Big)v_0=-\operatorname{Re}g_1u_0,\\ (L-\alpha^2)w_0=\alpha q_0,\quad (L-\alpha^2)\tau_0=\operatorname{Re}g_2u_0,\quad \frac{du_0}{dr}+\frac{u_0}{r}-\alpha w_0=0,\\ u_0=v_0=w_0=\tau_0=0\quad (r=1,R),\end{gathered}\tag{3.4}$$

where $L=\frac{d^2}{dr^2}+\frac{1-\varkappa}{r}\frac{d}{dr}$.

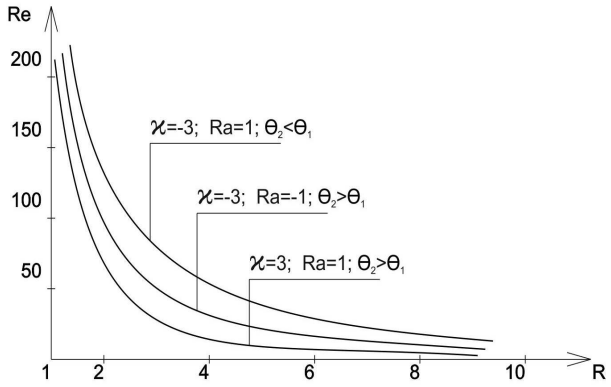

FIGURE 1. $\Omega=0$, $\mathrm{Pr}=0.7$.

The neutral curve corresponding to the bifurcation of azimuthal waves origination is found by solving the spectral problem

$$(\boldsymbol{M}-\operatorname{Re}\boldsymbol{N}-ic\operatorname{Re})\Phi_1=\nabla_1 p_1,\quad (\nabla_1,r\Phi_1)=0,\quad \Phi_1|_{r=1,R}=0.\tag{3.5}$$

A solution of problem (3.5) is sought for in the form

$$\Phi_1 = \{u_1(r), v_1(r), w_1(r), \tau_1(r)\} e^{-i(m\varphi+\alpha z)}, \quad p_1 = q_1(r) e^{-i(m\varphi+\alpha z)}, \quad (3.6)$$

where c is the unknown frequency of autooscillations, m is the azimuthal wave number.

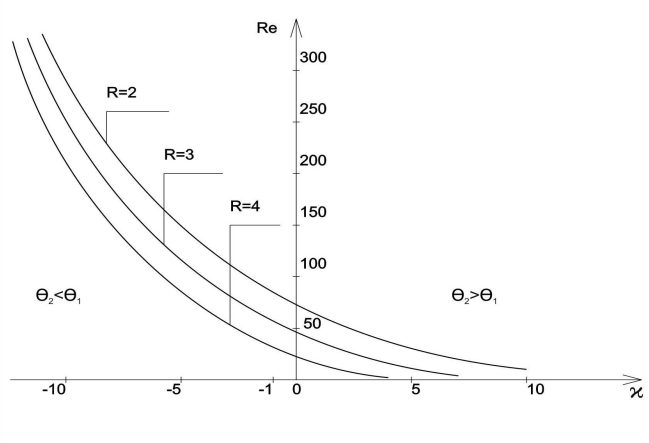

FIGURE 2. $\Omega = 0$, $Ra = 1$, $\mathrm{Pr} = 0.7$.

The substitution of (3.6) into (3.5) gives, after dividing the variables in (3.5), the spectral problem for ordinary differential equations:

$$\begin{gathered}
\Big[L_1 - \frac{1-\varkappa}{r^2} - \alpha^2 - i\mathrm{Re}\,(c - m\omega_1)\Big] u_1 = \\
= \frac{dq_1}{dr} - 2\mathrm{Re}\,\omega_1 v_1 + \mathrm{Re}\,Ra\omega_2\tau_1 - \frac{2im}{r^2} v_1, \\
\Big[L_1 - \frac{1+\varkappa}{r^2} - \alpha^2 - i\mathrm{Re}\,(c - m\omega_1)\Big] v_1 = \\
= -\frac{im}{r} q_1 - \mathrm{Re}\, g_1(r) u_1 + \frac{2im}{r^2} u_1, \qquad (3.7) \\
\Big[L_1 - \alpha^2 - i\mathrm{Re}\,(c - m\omega_1)\Big] w_1 = -i\alpha q_1, \\
\Big[L_1 - \alpha^2 - i\mathrm{Re}\,\mathrm{Pr}\,(c - m\omega_1)\Big] \tau_1 = \mathrm{Re}\, g_2 u_1, \\
\frac{du_1}{dr} + \frac{u_1}{r} - \frac{im}{r} v - i\alpha w_1 = 0, \quad u_1 = v_1 = w_1 = \tau_1 = 0 \quad (r = 1, R),
\end{gathered}$$

where $L_1 = \frac{d^2}{dr^2} + \frac{1-\varkappa}{r}\frac{d}{dr} - \frac{m^2}{r^2}$.

For fixed $\varkappa$, α, R, m, Pr, Ra and Ω problems of eigenvalues (3.4) and (3.7) are reduced to the Cauchy problems for eight ordinary differential

equations of first kind with real and complex coefficients. Use is made of the shooting method together with Newton's method. Numerical minimization of the Reynolds number Re is performed with respect to the wave numbers m and α.

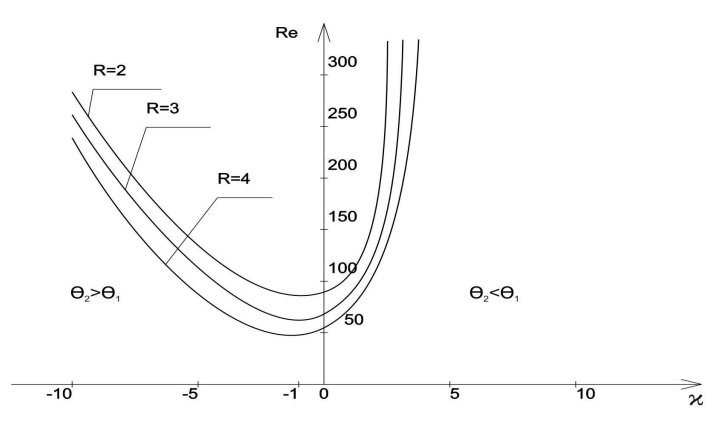

FIGURE 3. $\Omega = 0$, $Ra = -1$, $\mathrm{Pr} = 0.7$.

Figures 1–8 show the dependence of the minimized critical Reynolds number with respect to α (axial wave number)and m (azimuthal wave number) on the width of the gap between the cylinders when both axially symmetric and three-dimensional perturbations are considered for the fixed Rayleigh and radial Reynolds numbers. Here we are concerned with the cases where the outer cylinder is at rest ($\Omega = 0$), the cylinders rotate in the same direction for $\Omega = 0.2$, and the cylinders rotate in the opposite directions for $\Omega = -0.5$. The Prandtl number is $\mathrm{Pr} = 0.7$ for air and other gases and $\mathrm{Pr} = 7$ for water.

As seen in the figures, there are points and intervals on the curves, where the neutral curves of oscillatory modes with the azimuthal wave number $m = 1$ branch off the neutral curves with $m = 0$.

For $\mathrm{Pr} = 0.7$ Figure 1 presents the results of calculation of curves for $\Omega = 0$ (i.e. the cylinder is rest) for the concrete values of the radial Reynolds number $\varkappa$ with respect to the width of the gap between the cylinders. More exactly, for $\varkappa = -3$, $Ra = 1$ (the inward flow, $\Theta_2 < \Theta_1$), for $\varkappa = -3$, $Ra = -1$ (the inward flow, $\Theta_2 > \Theta_1$) and for $\varkappa = 3$, $Ra = 1$ (the outward flow, $\Theta_2 > \Theta_1$), destabilization of the main flow takes place as the gap width increases.

Thus, in the case of inward flow for $\Theta_2 > \Theta_1$ as well as for $\Theta_2 < \Theta_1$, we have a destabilizing effect. For the outward flow when the temperature

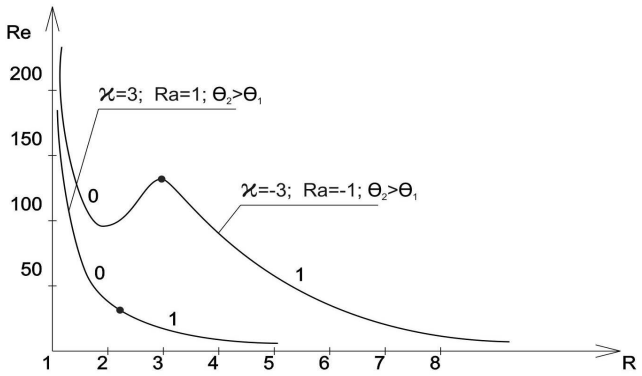

FIGURE 4. $\Omega = 0.2$, $\mathrm{Pr} = 0.7$.

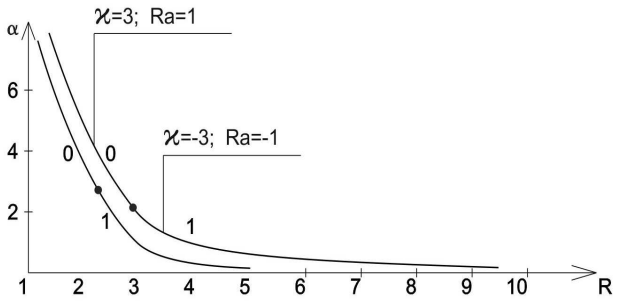

FIGURE 5. $\mathrm{Pr} = 0.7$, $\Omega = 0.2$, $\Theta_2 > \Theta_1$.

of the outer cylinders is greater than the temperature of the inner cylinder ($\Theta_2 > \Theta_1$), we observe destabilization of the main flow. Conversely, when the temperature of the inner cylinder is higher than the temperature of the outer cylinder ($\Theta_2 < \Theta_1$), the critical values of Re are sufficiently large (in

Figure 1 these values are not shown) and they are the larger, the greater the distance between the cylinders, and hence the flow is stable.

Figure 2 shows the dependence of critical values of Re on the $\varkappa$. As we see, for the outward flow as the parameter $\varkappa$ increases, the main flow gets destabilized and destabilization becomes stronger as the distance between the cylinders increases. For $\varkappa < 0$, when $|\varkappa|$ increases, the flow gets stabilized. The stabilizing effect becomes weaker as the distance between the cylinders increases.

Figure 3 presents the neutral curves for $Ra = -1$. In this case, for $\varkappa > 0$, $\Theta_2 < \Theta_1$, and for $\varkappa < 0$, $\Theta_2 > \Theta_1$, stabilization takes place as the gap between the cylinders decreases.

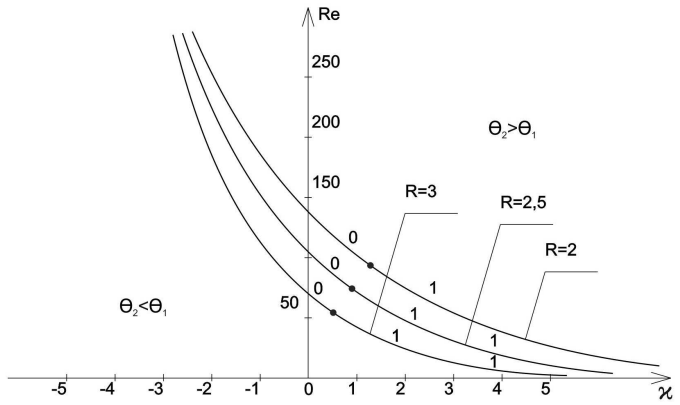

FIGURE 6. $\Omega = -0.5$, $Ra = 2$, $\mathrm{Pr} = 0.7$.

In all the above considered cases, stability loss occurs with axially symmetric perturbations.

Figure 4 presents the dependence of the minimized critical Reynolds numbers Re on the width of the gap between the cylinders for the concrete parameter values when the cylinders rotate in the same direction $\Omega = 0.2$. Then for $\varkappa = 3$, $Ra = 1$ and for $\varkappa = -3$, $Ra = -1$, the destabilizing effect takes place and the neutral curves of oscillatory instability with azimuthal wave number $m = 1$ branch off the neutral curve with $m = 0$ (the numbers 0,1 denote the minimized critical Reynolds number Re for $m = 0$ and for $m = 1$).

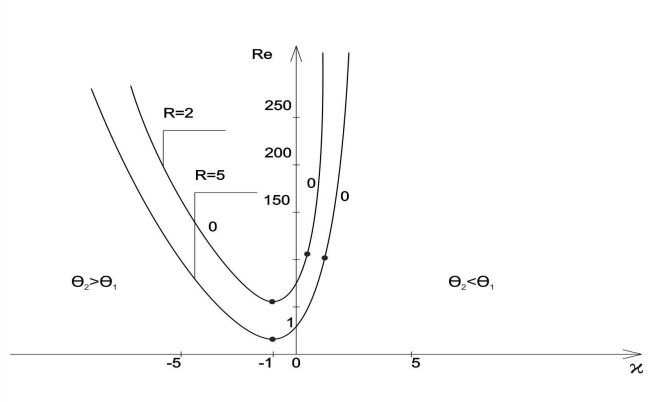

FIGURE 7. $\Omega = 0$, $\mathrm{Pr} = 7$, $Ra = -1$.

Figure 5 shows the dependence of the axial number on the width of a gap between the cylinders in the case where the cylinders rotate in the same direction. In such cases, as we see, as the gap between the cylinders increases the axial wave number decreases to 0, which testifies to the appearance of plane perturbations.

Figure 6 shows the neutral curves for the cylinders rotating in the opposite direction when $\Omega = -0.5$. For $\Theta_2 > \Theta_1$ and $\varkappa > 0$ there occurs destabilization which becomes more intensive as the distance between the cylinders increases. In this case, for certain values of the problem parameters, oscillatory perturbations branch off the rotational-symmetric neutral curve, which testifies to the appearance of oscillation regimes with period 2π. For $\varkappa < 0$ and $\Theta_2 < \Theta_1$, we observe motion stabilization which becomes more intensive as the distance between the cylinders decreases.

Figures 7 and 8 present the results of calculations for the Prandtl number $\mathrm{Pr} = 7$. Calculations were carried out when $\Omega = 0$ for $Ra = -1$ and for $Ra = 1$. As different from the case $\mathrm{Pr} = 0.7$, oscillation regimes with period 2π branch off the neutral curves for certain intervals of variation of $\varkappa$. In this case, the effect of stabilization weakening grows for the considered parameters of the problem as the Prandtl number and the distance between the cylinders increase.

4. Transition to Complex Regimes

The transition of the main flow (2.1) to complex regimes is considered in the neighborhood of the point of intersection of neutral curves corresponding to the axially symmetric and oscillation instability of the main stationary flow (2.1). Numerical studies were carried out by the methods which were

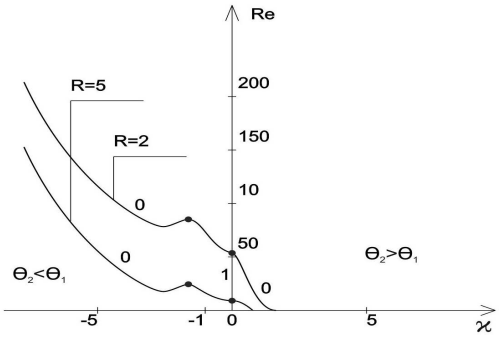

FIGURE 8. $\Omega = 0$, Pr $= 7$, $Ra = 1$.

used for studying the flow instability of various fluids (see [1], [4]–[6]) and the detailed description of which can be found in the book by [7].

The main object of the stability and bifurcation analysis is a dynamical system of amplitude equations which is a generalization of the Landau amplitude equation. The symmetry $\mathbf{G} = SO(2) \times O(2)$ makes it possible to split the system of amplitude equations into two subsystems, one of which is called the motor subsystem of modules ρ_0, ρ_1, ρ_2 and phase invariant $\beta = 2\psi_0 + \psi_1 - \psi_2$, and the other consists of phase equations:

$$\begin{aligned}
\dot\rho_0 =&\big[\sigma + A\rho_0^2 + B_r(\rho_1^2+\rho_2^2)\big]\rho_0 + D\rho_0\rho_1\rho_2\cos\beta,\\
\dot\rho_1 =&(\mu_r + P_r\rho_0^2 + Q_r\rho_1^2 + R_r\rho_1^2)\rho_1 + (S_r\cos\beta + S_i\sin\beta)\rho_0^2\rho_2,\\
\dot\rho_2 =&(\mu_r + P_r\rho_0^2 + R_r\rho_1^2 + Q_r\rho_2^2)\rho_2 + (S_r\cos\beta - S_i\sin\beta)\rho_0^2\rho_1,\\
\dot\beta =&C(\rho_1^2-\rho_2^2) - 2D\rho_1\rho_2\sin\beta -\\
&-\big[S_i(\rho_1^2-\rho_2^2)\cos\beta + S_r(\rho_1^2+\rho_2^2)\sin\beta\big]\rho_0^2/\rho_1\rho_2,\\
C =&2B_i + Q_i - R_i
\end{aligned} \tag{4.1}$$

where r denotes the real and i the imaginary part of a complex value. Phase equations have the form

$$\begin{aligned}
\dot\psi_0 =&B_i(\rho_1^2-\rho_2^2) - D\rho_1\rho_2\sin\beta,\\
\dot\psi_1 =&\mu_i + P_i\rho_0^2 + Q_i\rho_1^2 + R_i\rho_2^2 + (S_i\cos\beta - S_r\sin\beta)\rho_0^2\rho_2/\rho_1,\\
\dot\psi_2 =&\mu_i + P_i\rho_0^2 + R_i\rho_1^2 + Q_i\rho_2^2 + (S_i\cos\beta + S_r\sin\beta)\rho_0^2\rho_1/\rho_2,
\end{aligned} \tag{4.2}$$

where A, D are the real and B, P, Q, R, S the complex coefficients. σ and $\mu_r + i\mu_i$ are the damping decrements of axially symmetric stationary and oscillation perturbations, respectively. System (4.1) is invariant with respect to the transformation $\rho_1 \leftrightarrow \rho_2, \beta \leftrightarrow -\beta$, which is a consequence of the

invariance of the problem, with respect to the inversion J. Hence solutions of system (4.1) are either J-symmetric (transformed to themselves by the transformations $\rho_1 \leftrightarrow \rho_2, \beta \leftrightarrow -\beta$) or they generate J-connected pairs (transformed to each other).

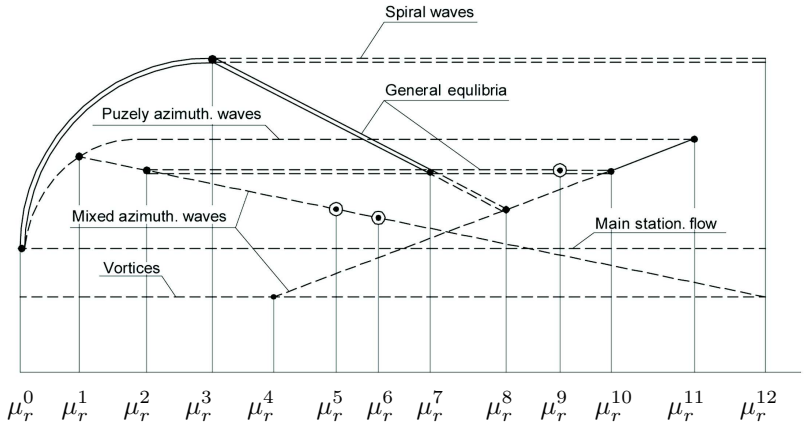

FIGURE 9. $R = 2$, Pr $= 7$. Bifurcation values: $\mu_r^0 = 0$, $\mu_r^1 = 355.6$, $\mu_r^2 = 392.5$, $\mu_r^3 = 609.28$, $\mu_r^4 = 4803.5$, $\mu_r^5 = 4870$, $\mu_r^6 = 4888.01$, $\mu_r^7 = 4915.5$, $\mu_r^8 = 5026.9$, $\mu_r^9 = 6700$, $\mu_r^{10} = 6871.5$, $\mu_r^{11} = 8969.5$, $\mu_r^{12} = 9450.9$.

The coefficients A, D, B, P, Q, R, P are defined in terms of eigensolutions of the linear problems (3.2) and (3.4) and their conjugates, also in terms of solutions of nonhomogeneous systems of ordinary differential equations whose right-hand sides depend on Φ_0, Φ_1.

Equilibria of the motor subsystem correspond to the fluid motions having the concrete physical nature. They can be found by analytical methods and be divided into two groups: equilibria lying on the invariant subspaces and equilibria of a general state. For the detailed analysis of stability and bifurcation of these equilibria see [7]. Following this monograph, the system of amplitude equations has the following types of equilibria:

(a) The main flow : $\rho_0 = \rho_1 = \rho_2 = 0$ for any β;

(b) Vortices : $\rho_0^2 = -\sigma/A$, $\rho_1 = \rho_2 = 0$ for any β;

(c) Purely azimuthal waves: $\rho_0 = 0$, $\rho_1^2 = \rho_2^2 = -\mu_r/(Q_r + R_r)$, for any β;

(d) Spiral waves: $\rho_0 = \rho_2 = 0$, $\rho_1^2 = -\mu_r/Q_r$, for any β,

$\rho_0 = \rho_1 = 0$, $\rho_2^2 = -\mu_r/Q_r$, for any β;

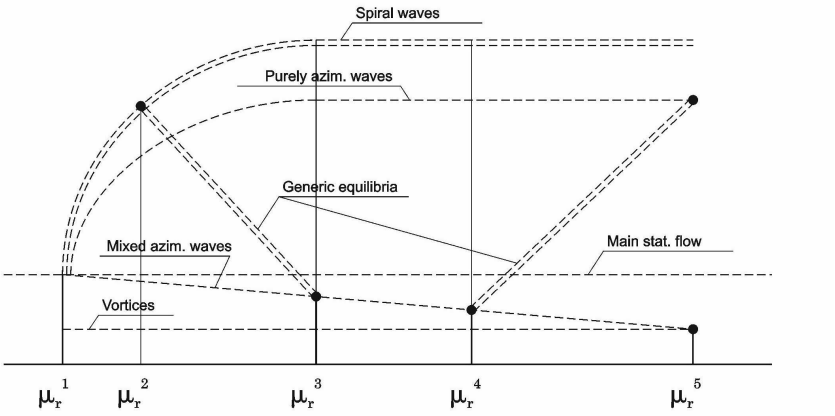

FIGURE 10. $R = 2.24$, $\mathrm{Pr} = 7$, $\sigma = 10$, $Re = 203.16$, $Ra = 2$, $\varkappa = -5$, $m = 1$, $\alpha = 3$, $\Omega = -0.0956$, $c = 0.2408$. Bifurcation values: $\mu_r^1 = 700.01$, $\mu_r^2 = 703.08$, $\mu_r^3 = 750.4$, $\mu_r^4 = 765.74$, $\mu_r^5 = 780.25$.

(e) A pair of mixed azimuthal waves:

$$\rho_0^2 = \Delta_1^+/\Delta^+, \quad \rho_1^2 = \rho_2^2 = \Delta_2^+/\Delta^+, \quad \beta = 0,$$
$$\rho_0^2 = \Delta_1^-/\Delta^-, \quad \rho_1^2 = \rho_2^2 = \Delta_2^-/\Delta^-, \quad \beta = \pi,$$
$$\Delta_1^+ = \sigma(Q_r + R_r) - \mu_r(2B_r + D), \quad \Delta_2^+ = \mu_r A - \sigma(P_r + S_r),$$
$$\Delta_1^- = \sigma(Q_r + R_r) - \mu_r(2B_r - D), \quad \Delta_2^- = \mu_r A - \sigma(P_r - S_r),$$
$$\Delta^+ = (2B_r + D)(P_r + S_r) - A(Q_r + R_r),$$
$$\Delta^- = (2B_r - D)(P_r - S_r) - A(Q_r + R_r).$$

In addition to the above-listed equilibria corresponding to the concrete flow regimes, the motor subsystem (4.1) may have equilibria not lying on its invariant subspaces, i.e., equilibria of a general state. Each of them corresponds to a quasi-periodic two-frequency solution of the amplitude system of equations.

In order to calculate the coefficients of the amplitude system, first we have to define the intersection points of neutral curves corresponding to the axially symmetric and oscillation loss of stability of the main flow. Simultaneously, we find the eigenvector-functions of the linear spectral problems and the eigenvector-functions of the conjugate problems. After that the solutions of eight linear nonhomogeneous boundary value problems are found.

At the final step of calculations, we find the functionals by means of which the amplitude system coefficients are expressed [7].

We present here several schemes of equilibria bifurcations of the main flow obtained for different values of the radius R (Figures 9–11).On these Figures the single lines show J-symmetric equilibria, the double lines J-connected pairs of equilibria. Stable equilibria are depicted by solid lines and unstable equilibria by dashed lines. The circles are points at which the motor subsystem cycles bifurcate.

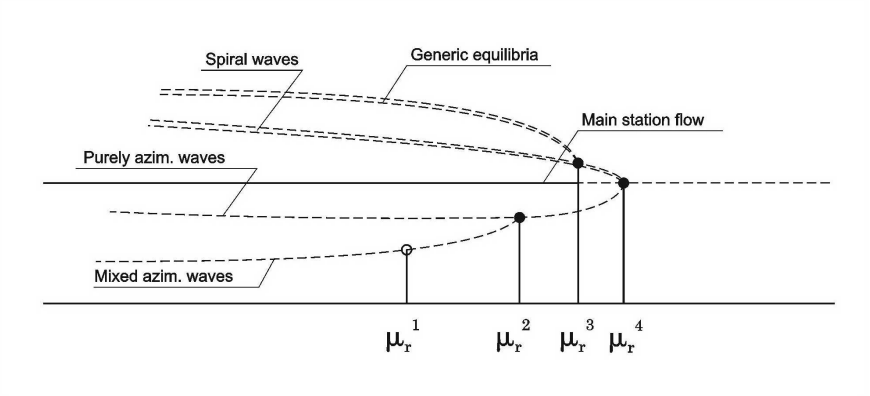

FIGURE 11. $R = 3$, $\mathrm{Pr} = 0.7$, $\sigma = -10$, $Re = 97.564$, $Ra = -2$, $\varkappa = -3$, $m = 1$, $\alpha = 2.5$, $\Omega = -0.1047$, $c = 0.2239$. Bifurcation values: $\mu_r^1 = -5.162$, $\mu_r^2 = -4.91$, $\mu_r^3 = -0.6919$, $\mu_r^4 = 0$.

Figure 9 show the scheme of transition to complex regimes for $\mathrm{Pr} = 7$, $R = 2$ (radius of the outer cylinder is twice as that of the inner cylinder) [1]. We present this scheme, where μ_r^0 - μ_r^{12} are bifurcation values, to compare it the schemes with the parameter R having other values.

Figure 10 shows transitions when $R = 2.24$ for the same parameters Pr, $\varkappa$, Ra, α, m as those used in the case $R = 2$. It turns out that the scheme of transitions is simpler than in the case $R = 2$ and becomes even simpler as the gap value increases. The number of bifurcation points decreases, all equilibria branching off the main stationary flow are unstable. Thus, immediately after the main flow loses stability there arise sufficiently complex motions of the fluid.

Figure 11 shows the scheme of transitions for $\mathrm{Pr} = 0.7$, $R = 3$. In this case, the main stationary flow itself turns out to be the only stable equilibrium. It loses stability for $\mu_r^4 = 0$ and, as a result, unstable spiral and azimuthal waves bifurcate from it, while at the point $\mu_r^1 = -5.17$ there

occurs the bifurcation of a cycle shaped like the figure eight [1] which further does not bifurcate.

5. Conclusions

The paper presents the results of the numerical analysis of the instability and bifurcations of flows between two porous heated cylinders with a superposed radial flow and a radial temperature gradient for different widths of the gap between the cylinders.

Figures 1–8 show that, depending on the parameters of the problem, with an increase of the gap width there occurs destabilization of fluid flow (2.1). Note that the larger the Prandtl number value, the more intensive the weakening effect of the stabilizing action of the problem parameters.

The picture of transitions to complex regimes in the motor subsystem becomes simpler with an increase of the distance between the cylinders (Figures 9–11). A characteristic feature is the absence of bifurcations of cycles of the motor subsystem from its equilibria and also the absence of stable equilibria for any values of the parameters, which testifies to quick transitions to complex regimes.

References

1. V. V. Kolesov and L. D. Shapakidze, Instabilities and transition in flows between two porous concentric cylinders with radial flow and a radial temperature gradient. *Physics of Fluids* **23** (2011), 014107–1–014107–13.
2. L. D. Landau and E. M. Lifshits, Fluid Mechanics. *Butterworth - Heinemann*, 1987.
3. G. Gersshuni and E. Zhukhovitski, Convective stability of incompressible fluid. *Keter Publications*, Jerusalem/Wiley, 1976.
4. V. V. Kolesov and L. D. Shapakidze, On oscillatory modes in viscous incompressible liquid flows between two counter-rotating permeable cylinders. In Trends in applications of mathematics to mechanics, *Proceedings of the international conference STAMM* 98*,* 11*th symposium, Univ. of Nice, Nice, France*, 1998, *CRC Press. Chapman Hall/CRC Monogr. Surv. Pure Appl. Math.* **106** (2000), 221–227.
5. V. V. Kolesov and V. I. Yudovich, Calculation of oscillatory regimes in Couette flow in the neighborhood of the point of intersection of bifurcations initiating Taylor vortices and azimuthal waves. *Fluid Dyn.* **33** (1998), No. 4, 532–542.
6. V. V. Kolesov and A. G. Khoperskiĭ, Simple regimes of fluid motion in the neighborhood of the intersection of bifurcations initiating nonisothermal Taylor vortices and azimuthal waves. *Fluid Dyn.* **37** (2002), No. 2, 257–267.
7. V. V. Kolesov and A. G. Khoperskiĭ, Nonisothermal Couette - Taylor's Problem. (Russian) *Rostov, Yuj. Fed. Yniv.*, 2009.

(Received 2.11.2011)

Author's address:

A. Razmadze Mathematical Institute
I. Javakhishvili Tbilisi State University
2, University Str., Tbilisi 0186
Georgia